Pathology after combined epicardial and endocardial ablation for ventricular tachycardia in a postmortem heart with hypertrophic cardiomyopathy

Kenzaburo Nakajima, MD,[*] Koji Miyamoto, MD, PhD,[*] Taka-aki Matsuyama, MD, PhD,[†] Takashi Noda, MD, PhD,[*] Hatsue Ishibashi-Ueda, MD, PhD,[†] Kengo Kusano, MD, PhD[*]

From the [*]Department of Cardiovascular Medicine, National Cerebral and Cardiovascular Center, Osaka, Japan, and [†]Department of Pathology, National Cerebral and Cardiovascular Center, Osaka, Japan.

Introduction

Ventricular arrhythmias in patients with nonischemic cardiomyopathy (NICM) often affect patients' prognosis. Ventricular tachycardias (VTs) arising from the electrical scar area in hearts of NICM patients could become targets for radiofrequency catheter ablation (RFCA) therapy.[1–3] However, the efficacy of RFCA using the endocardial approach is limited because of the deeper localization of the electrical scar from the intramural to the epicardial side.[1–3] Recently, combined endocardial and epicardial ablation has been used to improve the RFCA outcomes for VT in patients with NICM. However, elimination of the VTs is still challenging,[1–6] especially in patients with hypertrophic cardiomyopathy (HCM).[7,8] In this case report, we evaluated the pathologic features after combined epicardial and endocardial ablation in a postmortem heart from a patient with HCM.

Case report

The patient was a 73-year-old man who was diagnosed with HCM at the age of 63 years. The left ventricular chamber showed progressive dilation with contractile dysfunction from the age of 67, and the heart was thought to be in an advanced dilated form. In spite of the administration of β-blocker and amiodarone as concomitant medical therapy for heart failure and nonsustained VT, the effect was insufficient, and he was implanted with cardiac resynchronization therapy with defibrillator.

KEYWORDS Hypertrophic cardiomyopathy; Pathology; Ablation; Ventricular tachycardia

ABBREVIATIONS **ECG** = electrocardiogram; **HCM** = hypertrophic cardiomyopathy; **LV** = left ventricle; **LVZ** = low-voltage zone; **NICM** = nonischemic cardiomyopathy; **RF** = radiofrequency; **RFCA** = radiofrequency catheter ablation; **VT** = ventricular tachycardia

(Heart Rhythm Case Reports 2015;1:310–314)

Address reprint requests and correspondence: Koji Miyamoto, MD, Department of Cardiovascular Medicine, National Cerebral and Cardiovascular Center, 5-7-1 Fujishirodai Suita, Osaka, 565-8565, Japan. E-mail address: miyamoto.koji.hp@ncvc.go.jp.

The patient was admitted to our hospital because of repetitive drug-resistant VT at the age of 73 years. Echocardiography revealed an aneurysm at the apical portion of the left ventricle (LV), which was accompanied by severe LV dysfunction (left ventricular ejection fraction 21%) and asymmetric septal hypertrophy. On the day of admission, the patient presented with VT storm, was intubated, and underwent assisted cardiopulmonary support because the VTs were resistant to antiarrhythmic drugs and hemodynamically unstable. Coronary angiography showed no significant stenosis in coronary arteries. Under intravenous β-blocker administration, RFCA was performed to control the VT storm.

Electrophysiological examination and ablation procedure

Most of the clinical VTs in the 12-lead electrocardiogram (ECG) showed a right bundle branch block pattern with slowed initial precordial QRS activation (Figure 1A). We performed RFCA using the epicardial and endocardial approach because the origins of some VTs were thought to be located on the epicardial side based on the 12-lead ECG findings.

Steerable catheters were inserted from the right femoral vein and placed in the coronary sinus and the ventricle of interest. The LV endocardium was accessed using the transseptal approach. Pericardial access was obtained through a subxiphoid and anterior puncture under fluoroscopic guide.

We used a 3.5-mm open-irrigatedtip ablation catheter, Thermocool (Biosense Webster, Johnson & Johnson, Diamond Bar, CA), which was also used for mapping. Bipolar voltage maps of the endocardium and epicardium were constructed during sinus rhythm. Arrhythmogenic areas, indicated by low-voltage zones (LVZs), which were defined as <1.5 mV at the endocardium and <1.0 mV at the epicardium, were mainly located on the lateral to posterior wall in the LV endocardium and throughout the entire LV in the epicardium (Figure 2A and B).

http://dx.doi.org/10.1016/j.hrcr.2015.04.003

KEY TEACHING POINTS

- Lesion depth created by radiofrequency catheter ablation is smaller on the epicardium with adipose tissue than on the endocardium.
- It seems to be difficult to create transmural lesions even by combined epicardial and endocardial ablation, especially in patients with thickened ventricular walls.
- Some approaches such as needle, bipolar, and transcoronary ethanol ablation may be more effective to create transmural lesions.

Six forms of VTs were induced by right ventricular pacing, although clinically documented VTs did not appear (Figure 1B). We performed substrate-based RFCA, which targeted the LVZs and abnormal electrograms such as delayed potentials, fragmented potentials, and/or double potentials in the endocardium and epicardium. Open-irrigated radiofrequency (RF) current was delivered for up to 60 seconds in power-controlled mode as follows: power 30–45 W and irrigation 17–30 mL/min. Total application time of RFCA was about 86 minutes.

Clinical course after ablation

A VT that was not induced in the electrophysiological study emerged after the RFCA session. The VT was clinically controlled by antiarrhythmic drugs (amiodarone, nifekalant, and lidocaine). The patient, however, died from deterioration of heart failure 49 days after the procedure. A postmortem examination of the heart was performed.

Postmortem gross pathologic findings

The epicardium of the heart was mildly adhered to the pericardium around the apex of the LV with a thin fibrinous exudate, and this was thought to be an inflammatory reaction after the epicardial ablation procedure. There was no increase in pericardial fluid volume.

The heart was significantly enlarged and weighed 820 g. There was rich epicardial fat attached in the atrioventricular and interventricular groove, and it was also widely distributed in the free wall of the LV that roughly corresponded to the voltage map findings (Figure 2B and C). On the LV epicardial surface, RFCA results showed discolored spotty lesions around the LV apex.

All 4 chambers of the heart were dilated along the long axis section through the heart. The LV wall showed asymmetric hypertrophy as follows: 27 mm thickness in the ventricular septum, and the papillary muscle was also hypertrophied (Figure 3A). The LV apical wall was thinning with complex endocardial trabeculation, and it showed aneurysmal dilation that was thought to be an arrhythmogenic source. The ablated lesions from the endocardial approach were observed as blackish spots mainly located in and at the border of the aneurysmal lesion. All coronary arteries showed no arteriosclerotic stenosis.

Ablated lesion beneath the epicardium and endocardium

Figure 3 shows a cross section of the ablated lesions at the border of the LV aneurysm, where both the epicardial and endocardial approach ablation lesions were assessed. The endocardial lesions were clearly defined and were deeper than the epicardial lesions. The cloudy discolored areas were necrotic tissue caused by RF energy, and the adjacent black-colored areas were lesions with hemorrhage caused by

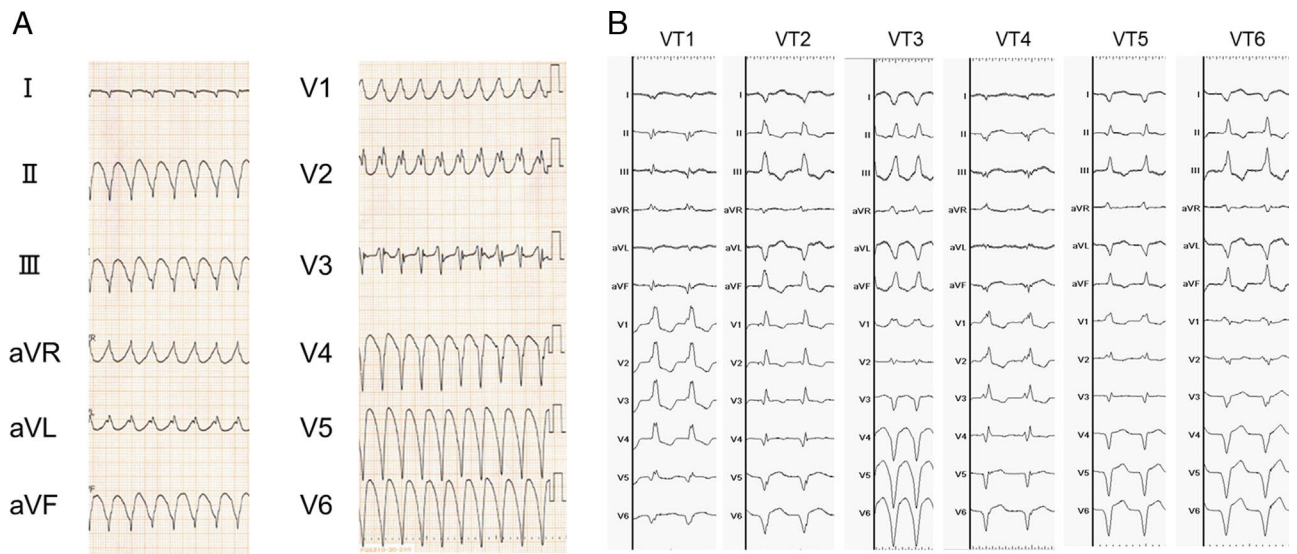

Figure 1 **A:** A representative 12-lead electrocardiogram of clinical ventricular tachycardia (VT). The VT exhibited a right bundle branch block pattern and a right superior axis. VT cycle length is 330 ms, with a widened QRS duration and a slowed initial precordial QRS activation, indicating that the VT is of epicardial origin. **B:** Six VTs induced by right ventricular pacing.

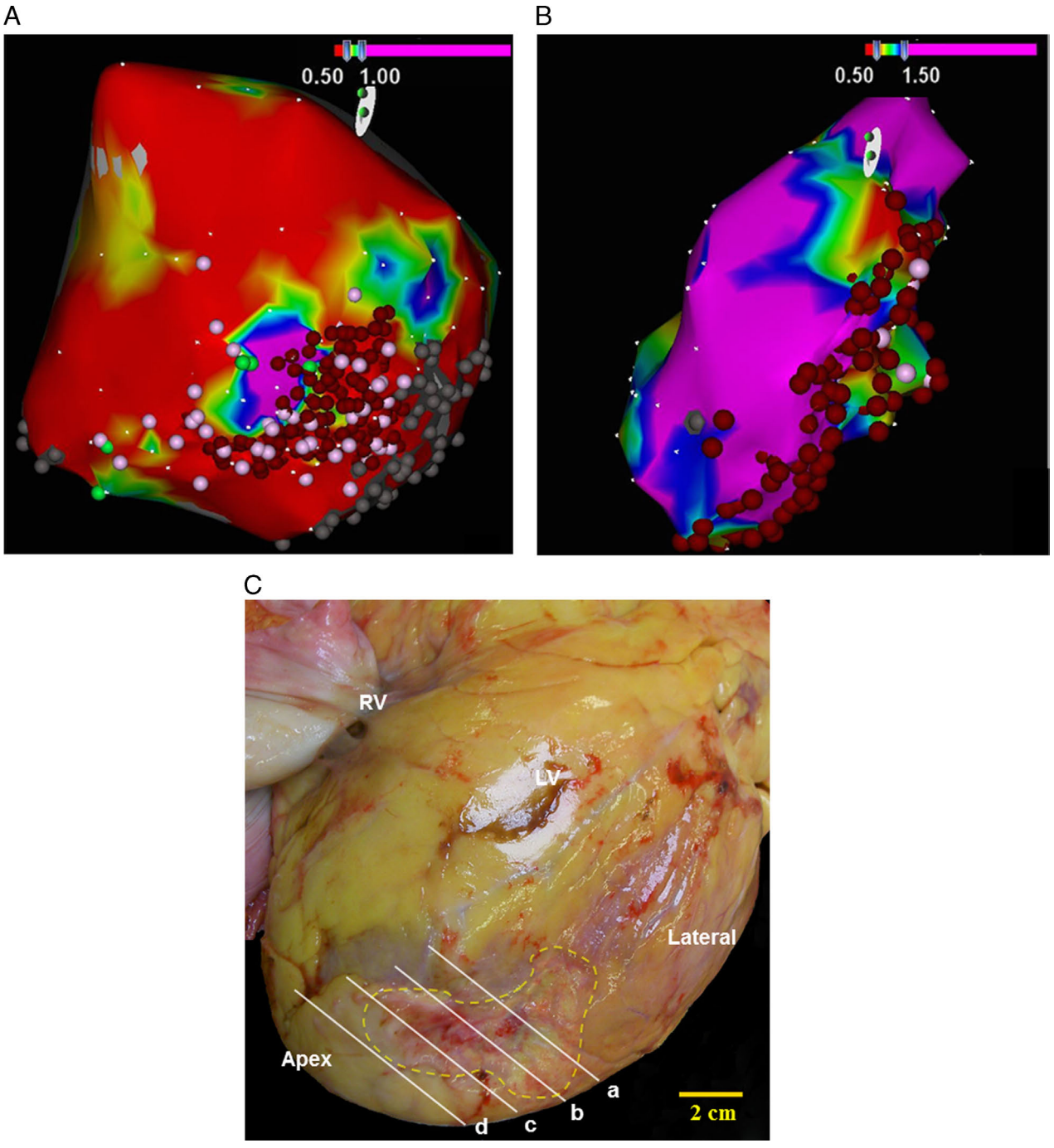

Figure 2 Comparison between the macroscopic view of the epicardial surface and the electroanatomic voltage map. **A:** Epicardial voltage map of the left ventricle (LV) from the left lateral cranial direction. Blue, green, yellow, and red areas indicate the progressively low-voltage zones (LVZs), defined as <1.0 mV. Brown dots indicate ablation points. Pink dots indicate abnormal electrocardiograms including the delayed potentials, fragmented potentials, and double potentials. **B:** Endocardial voltage map of the LV from the left lateral cranial direction. Brown dots indicate ablation points. The LVZ, defined as <1.5 mV, is located lateral to the posterior wall in the LV endocardium. **C:** The macroscopic view of the LV corresponds to Figure 2A before fixation in formalin. Rich adipose tissue covers the epicardial surface. The opaque discolored yellow area encircled by the dotted line indicates the ablation lesion. The location of the fatty tissue and uncovered myocardium roughly corresponds to the findings of epicardial voltage map. The white line labeled b indicates the cutting line in Figure 3B. Microscopic findings at lines a, c, and d are shown in the Supplemental Figure (available online). RV = right ventricle.

damage to intramural small coronary arteries and capillaries. On the epicardial side, the LV apex around the ablated lesions was diffusely covered by fatty tissue, and its thickness was up to 5 mm. The fatty layer was transmurally discolored; however, the change of the myocardium beneath the epicardial fat was limited (Figure 3B).

Figure 3C shows the identical histologic sections to Figure 3B, and the original pathologic fibrosis resulting from HCM diffusely extended mainly in the center and epicardial side of the LV wall. The ablation scar reached a depth of 6 mm from the endocardial surface at its deepest site, whereas the ablation scar from the epicardial surface

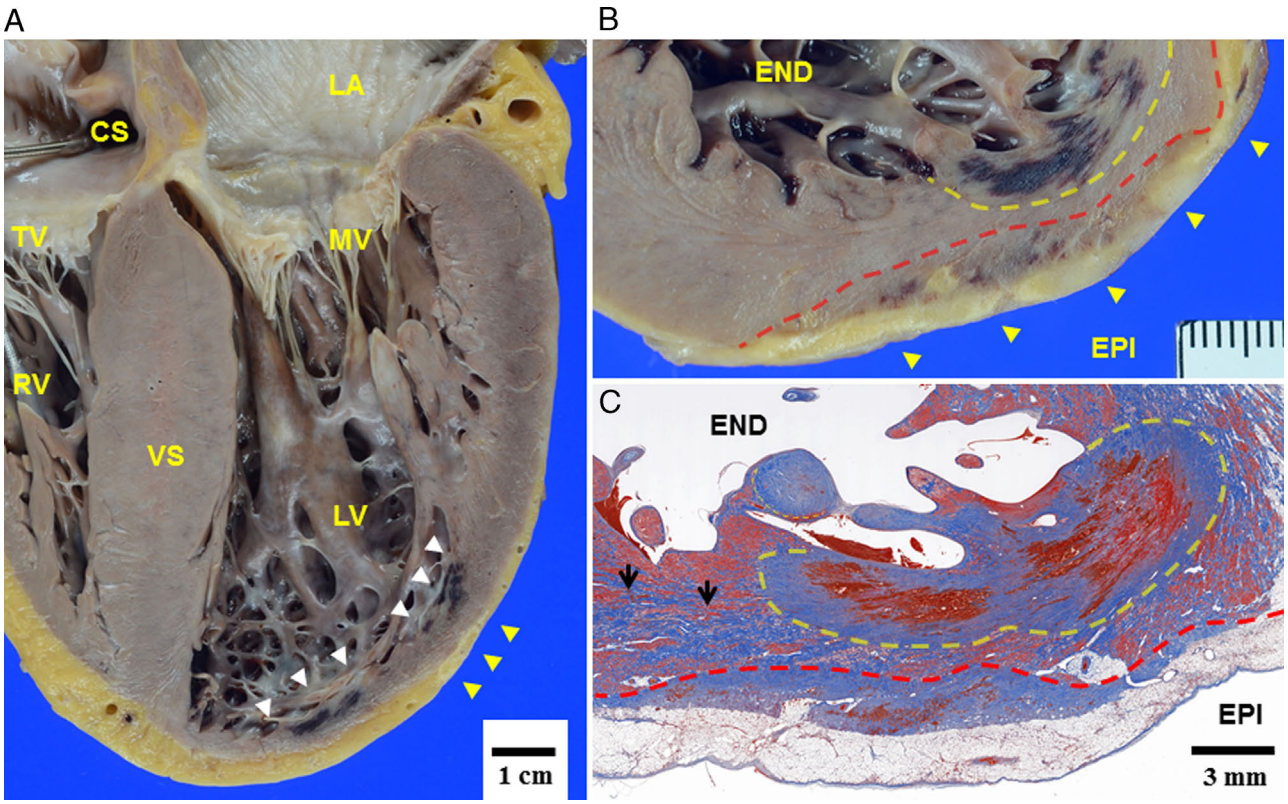

Figure 3 Cross sections of the ablated lesions, post formalin fixation. **A:** Macroscopic endocardial overview of the left ventricle (LV) in the 4-chamber cut. The ventricular septum (VS) shows asymmetric hypertrophy, and the apex shows aneurysmal dilation with the wall thinning. Ablated lesions (*white and yellow arrowheads*) are located in the dilated lesion. **B:** Cross-sectional macroscopic finding at the white line in Figure 2C. *Yellow arrowheads* indicate ablated lesions in epicardial fat, which is approximately 2–4 mm thick. Blackish areas are observed at deeper sites in the endocardium. **C:** Microscopic findings from Figure 3B with Masson's trichrome stain. Irregular fibrotic layers that are originally caused by hypertrophic cardiomyopathy (HCM) are mainly distributed in the center of the LV wall (*black arrows*). The yellow dotted line represents an ablation lesion from the endocardium. Within this area, hemorrhagic necrosis is observed. The red line represents an ablation lesion from the epicardium, and the ablation scar reached a maximum depth of 6 mm. On the epicardium, the maximum depth of the ablation scar was only 2 mm beyond the epicardial adipose tissue. Myocardium that escaped the ablation energy was visible between the epicardial and endocardial ablation lesions. CS = coronary sinus, LA = left atrium, TV = tricuspid valve, RV = right ventricle, MV = mitral valve, END = endocardium, EPI = epicardium.

reached only 2 mm beyond the epicardial fat. Between the epicardial and endocardial ablated lesions, there was approximately 1.5 mm of viable myocardial tissue with pathologic fibrosis that escaped the RF energy at the border of the aneurysmal wall, and there were no obvious transmural ablation lesions. In addition, the spared viable myocardium was especially noted on the top of the trabeculi or bridging the myocardial bundles, despite that the deeper sites were ablated.

The peripheral area of the ablated sites was replaced with mature fibrous tissue, but the remaining necrotic tissue and hemorrhagic area were still observed at the core of the ablated sites. This histologic discrepancy in the relatively long phase after RF (approximately 6 weeks) may be attributed to the prolonged wound healing process of the intramural hemorrhage and small vessel injuries.[9]

Discussion

This case provided us with important information by the analysis of pathologic changes after combined epicardial and endocardial ablation with open-irrigated catheter for the first time in a human heart. We focused on the 2 major findings in this heart, as described below.

The finding of voltage maps with larger LVZ on the epicardium than that on the endocardium was roughly in accordance with the histopathology of the heart (Figure 3C and Supplemental Figure, available online). We assumed that the LVZ on the epicardium, however, indicated not only original pathologic fibrosis but also the fat on the epicardium. The pathologic evaluation showed that transmural ablation could not be achieved in this case. Even though new strategies such as local abnormal ventricular activity ablation or homogenization of the scar area in electroanatomic mapping have been developed for unstable hemodynamic VTs, efficacy of epicardial ablation is limited in cases like this, which might be attributed to residual arrhythmic substrate, especially in NICM.[10,11] The saline irrigation catheter produces deeper and larger ablation lesions in vivo compared with a non–irrigation catheter.[12] However, despite the use of open-irrigated epicardial ablation, transmural ablation lesions are found in only 55% of cases.[13]

Some studies reported that the lesions made by epicardial ablations were affected by the rich adipose tissues in the

epicardium.[14] The degree of influence of the epicardial fat thickness on the RF delivery is controversial. Van Huls van Taxis et al[15] reported the clear cut-off of thickness threshold to impair RF delivery as 7 mm. On the other hand, Hong et al[16] reported that the epicardial fat could severely limit the lesion depth created by RF energy, even in the case with the epicardial fat thickness of 2 mm.[16] In this case, ablated scars were not reached deeper from epicardial site than those from endocardial site because of rich adipose tissues. The impaired RF delivery, which was demonstrated by limited ablation lesions from the epicardial surface, might also result from the catheter instability, weak contact force, and/or inadequate RF power on the epicardium. The VT recurrence after RFCA might be also due to inability to map and/or identify critical sites of VTs. We retrospectively examined the electrogram response (R wave reduction of the electrogram) by RF delivery in this case, and compared it between RF delivery from the epicardium and from the endocardium. In total, the number of RF applications from the endocardium was 128 and that from the epicardium was 109. The mean percentage of the R wave reduction by RF energy was significantly lower in the epicardium than in the endocardium (59% ± 25% vs 69% ± 25%; $P = .009$). In order to achieve transmural lesions, other approaches such as needle, bipolar, and transcoronary ethanol ablation may be necessary, especially in cases with thickened ventricular wall, as in this HCM patient.[17–19]

In this case, we could control VTs clinically with concomitant use of antiarrhythmic drugs. Therefore, combined epicardial and endocardial ablation was useful to modify the substrate for VTs in spite of the residual viable myocardial tissue between the endocardium and epicardium in this case.

Conclusion

To our knowledge, this is the first case that shows important pathologic information after combined epicardial and endocardial ablation using an open-irrigated catheter in a human heart. This pathologic report showed the limitation of the epicardial RFCA to deliver sufficient RF energy to the myocardium beyond the epicardial adipose tissue, which resulted in residual arrhythmogenic substrate even after combined epicardial and endocardial RFCA.

Appendix

Supplementary data

Supplementary data associated with this article can be found in the online version at http://dx.doi.org/10.1016/j.hrcr.2015.04.003.

References

1. Soejima K, Stevenson WG, Sapp JL, Selwyn AP, Couper G, Epstein LM. Endocardial and epicardial radiofrequency ablation of ventricular tachycardia associated with dilated cardiomyopathy: the importance of low-voltage scars. J Am Coll Cardiol 2004;43:1834–1842.
2. Desjardins B, Yokokawa M, Good E, Crawford T, Latchamsetty R, Jongnarangsin K, Ghanbari H, Oral H, Pelosi F Jr, Chugh A, Morady F, Bogun F. Characteristics of intramural scar in patients with nonischemic cardiomyopathy and relation to intramural ventricular arrhythmias. Circ Arrhythm Electrophysiol 2013;6:891–897.
3. De Cobelli F, Pieroni M, Esposito A, Chimenti C, Belloni E, Mellone R, Canu T, Perseghin G, Gaudio C, Maseri A, Frustaci A, Del Maschio A. Delayed gadolinium-enhanced cardiac magnetic resonance in patients with chronic myocarditis presenting with heart failure or recurrent arrhythmias. J Am Coll Cardiol 2006;47:1649–1654.
4. Sosa E, Scanavacca M, D'avila A, Pilleggi F. A new technique to perform epicardial mapping in the electrophysiology laboratory. J Cardiovasc Electrophysiol 1996;7:531–536.
5. Maury P, Escourrou G, Guilbeau C, Duparc A, Hebrard A, Delay M. Histopathologic effects of endocardial and epicardial percutaneous radiofrequency catheter ablation in dilated nonischemic cardiomyopathy. Pacing Clin Electrophysiol 2008;31:1218–1222.
6. Santangeli P, Di Biase L, Lakkireddy D, et al. Radiofrequency catheter ablation of ventricular arrhythmias in patients with hypertrophic cardiomyopathy: safety and feasibility. Heart Rhythm 2010;7:1036–1042.
7. Dukkipati SR, d'Avila A, Soejima K, Bala R, Inada K, Singh S, Stevenson WG, Marchlinski FE, Reddy VY. Long-term outcomes of combined epicardial and endocardial ablation of monomorphic ventricular tachycardia related to hypertrophic cardiomyopathy. Circ Arrhythm Electrophysiol 2011;4:185–194.
8. Inada K, Seiler J, Roberts-Thomson KC, Steven D, Rosman J, John RM, Sobieszczyk P, Stevenson WG, Tedrow UB. Substrate characterization and catheter ablation for monomorphic ventricular tachycardia in patients with apical hypertrophic cardiomyopathy. J Cardiovasc Electrophysiol 2011;22:41–48.
9. Delacatretaz E, Stevenson WG, Winters GL, et al. Ablation of ventricular tachycardia with a saline-cooled radiofrequency catheter: anatomic and histologic characteristics of the lesions in humans. J Cardiovasc Electrophysiol 1999;10:860–865.
10. Jaïs P, Maury P, Khairy P, et al. Elimination of local abnormal ventricular activities a new end point for substrate modification in patients with scar-related ventricular tachycardia. Circulation 2012;125:2184–2196.
11. Di Biase L, Santangeli P, Burkhardt DJ, et al. Endo-epicardial homogenization of the scar versus limited substrate ablation for the treatment of electrical storms in patients with ischemic cardiomyopathy. J Am Coll Cardiol 2012;60:132–141.
12. Nakagawa H, Yamanashi WS, Pitha JV, Arruda M, Wang X, Ohtomo K, Beckman KJ, McClelland JH, Lazzara R, Jackman WM. Comparison of in vivo tissue temperature profile and lesion geometry for radiofrequency ablation with a saline-irrigated electrode versus temperature control in a canine thigh muscle preparation. Circulation 1995;91:2264–2273.
13. Fenelon G, Pereira KP, de Paola AA. Epicardial radiofrequency ablation of ventricular myocardium: factors affecting lesion formation and damage to adjacent structures. J Interv Card Electrophysiol 2006;15:57–63.
14. Desjardins B, Morady F, Bogun F. Effect of epicardial fat on electroanatomical mapping and epicardial catheter ablation. J Am Coll Cardiol 2010;56:1320–1327.
15. van Huls van Taxis CF, Wijnmaalen AP, Piers SR, van der Geest RJ, Schalij MJ, Zeppenfeld K. Real-time integration of MDCT-derived coronary anatomy and epicardial fat: impact on epicardial electroanatomic mapping and ablation for ventricular arrhythmias. JACC Cardiovasc Imaging 2013;6:42–52.
16. Hong KN, Russo MJ, Liberman EA, Trzebucki A, Oz MC, Argenziano M, Williams MR. Effect of epicardial fat on ablation performance: a three-energy source comparison. J Card Surg 2007;22:521–524.
17. Sapp JL, Beeckler C, Pike R, Parkash R, Gray CJ, Zeppenfeld K, Kuriachan V, Stevenson WG. Initial human feasibility of infusion needle catheter ablation for refractory ventricular tachycardia. Circulation 2013;128:2289–2295.
18. Koruth JS, Dukkipati S, Miller MA, Neuzil P, d'Avila A, Reddy VY. Bipolar irrigated radiofrequency ablation: a therapeutic option for refractory intramural atrial and ventricular tachycardia circuits. Heart Rhythm 2012;9:1932–1941.
19. Tokuda M, Sobieszczyk P, Eisenhauer AC, Kojodjojo P, Inada K, Koplan BA, Michaud GF, John RM, Epstein LM, Sacher F, Stevenson WG, Tedrow UB. Transcoronary ethanol ablation for recurrent ventricular tachycardia after failed catheter ablation: an update. Circ Arrhythm Electrophysiol 2011;4:889–896.